We are IntechOpen, the world's leading publisher of Open Access books Built by scientists, for scientists

4,800
Open access books available

122,000
International authors and editors

135M
Downloads

Our authors are among the

154
Countries delivered to

TOP 1%
most cited scientists

12.2%
Contributors from top 500 universities

WEB OF SCIENCE™

Selection of our books indexed in the Book Citation Index in Web of Science™ Core Collection (BKCI)

Interested in publishing with us?
Contact book.department@intechopen.com

Numbers displayed above are based on latest data collected.
For more information visit www.intechopen.com

18

Dual Mode Microstrip Ring Resonator with Composite-Right/Left-handed Line

M.K.Haldar, Hieng Tiong Su and Kian Kiong Fong
Swinburne University of Technology (Sarawak Campus)
Sarawak, Malaysia

1. Introduction

Microwave and RF filters play an important role in various electronic systems, including cellular radio, satellite communications and radar. Filters are used in these systems in order to discriminate between wanted and unwanted signal frequencies. High performance filters are desirable for good signal reception and therefore for a better system performance. The demands for high performance filters are mainly due to the stringent frequency spectrum requirements following the emerging of new applications for modern communication systems. High performance filters are filters with low insertion loss, high frequency selectivity, phase linearity and potentially no harmonic response. Following the advancement of modern technologies, design considerations have been extended to achieve compact size and light-weight, making the filter design a more challenging task. Although enormous amount of literature on various filter theories is available, new filters are continually developed and reported in major journal and conference publications, to suit severe design specifications.

In general, microwave filters are divided into two broad classes, they are distributed type and lumped-element type. At microwave frequencies the use of distributed circuit elements in implementing passive microwave devices is widespread. They differ from lumped circuits as one or more dimensions are a significant fraction of the operating wavelength. Design formulae are available in many texts. Distributed filters can take the form of planar structures or waveguide cavity and they are preferable for high Q filter design. However, the latter has the advantage of low or no spurious harmonic responses.

In this chapter, we will give a new design perspective for a potentially high performance filter namely a dual-mode microstrip ring resonator with composite-right/left-handed (CRLH) line, for suppression of first harmonic. In section 2, we will first describe the terminologies of Left-Handed (LH) and Right-Handed (RH) transmission lines and show how their wave propagation properties are different using their transmission line models. In Section 3, we will give an overview of ring resonator's research, how ring resonator can be used in a single mode or a dual-mode resonator design.

In section 4, we will discuss the principle of operation of a composite-right/left-handed line ring resonator, and explain how harmonic supprssion can be achieved.

In sections 5, we will present the implementation of CRLH ring resonator. We will give the formulation use in the design and show how the left-handed line is incorporated into a ring resonator.
In section 6, we will take the circuit-modeling approach to analyse the CRLH ring resonator in greater details. This serves as initial design guidelines to quickly determine the filter layout dimensions, given a filter specification. The final design can then be simulated using commercial electromagnetic simulator. Some measurement results will be presented.
In section 7 and 8, we express other design considerations for the CRLH ring resonator and give suggestions for future developments.

2. Left and Right Hand Transmission Lines

The term left-handed transmission line is relatively new although such lines have long been known. The term comes from a speculative paper (Veselago, 1968), which considered the electromagnetic properties of a material with negative permittivity and permeability. Among other interesting properties, such a material will have a negative refractive index. However, it was many years later that experimentalists (Shelby et al, 2001) demonstrated such a material. These materials were called left-handed metamaterials.
Consider a uniform plane wave in a right-handed rectangular Cartesian coordinate system. The direction of the Poynting vector is always given by the direction of motion of a right-handed cork screw as it is rotated from the electric field vector to the magnetic field vector. Assuming the fields to vary as $e^{j\left(\omega t-\vec{k}\bullet\vec{r}\right)}$, where ω is the angular frequency (radians/s), t is time, $\vec{k}$ is the wave vector, $\vec{r}$ is the position vector, and $j=\sqrt{-1}$. Maxwell's curl equations can be written in the SI units as

$$\vec{k}\times\vec{E}=\omega\mu\vec{H} \tag{1}$$

$$\vec{k}\times\vec{H}=-\omega\varepsilon\vec{E} \tag{2}$$

where $\vec{E}$ and $\vec{H}$ represent the electric and magnetic field vectors and ε and μ are the permittivity and permeability of the medium considered to be isotropic.
These equations show that the wave vector, $\vec{k}$ is perpendicular to the electric and magnetic field vectors. If both ε and μ are positive, the direction of $\vec{k}$ is given by the direction of $\vec{E}\times\vec{H}$, i.e., the Poynting vector. The direction of the wave vector is therefore given by the direction of motion of a right-handed cork screw as it is rotated from the electric field vector to the magnetic field vector. Hence, such a medium is called right-handed. Most materials occurring in nature are right-handed. On the other hand, if both ε and μ are negative the direction of $\vec{k}$ is given by the direction of $-\vec{E}\times\vec{H}$, i.e., opposite to the direction of the Poynting vector. The direction of the wave vector is therefore given by the direction of motion of a left-handed cork screw as it is rotated from the electric field vector to the magnetic field vector. Hence, such a medium is called left-handed. The Poynting vector is associated with the direction of energy flow, while the wave vector represents the direction of motion of the wave fronts. The former therefore represents the direction of group velocity while the latter represents the direction of phase velocity. Hence the phase and group

velocities are in the same direction in a right-handed material and in opposite directions in a left-handed material. Waves with opposite directions of phase and group velocities have been known for a long time and have been used in backward wave oscillators. These waves travel in periodic structures and are called slow waves (Beck, 1958) because their phase velocities are less than the phase velocity of light in the medium in which these periodic structures are embedded.

It is a common practice in electrical engineering to model wave propagation by transmission line theory which can represent both slow and fast waves. Thus it is expected that a left-handed material can be represented by a transmission line. Fig.1 shows the transmission line model represented by a distributed series impedance, Z Ohms/m and a distributed shunt admittance, Y Siemens/m.

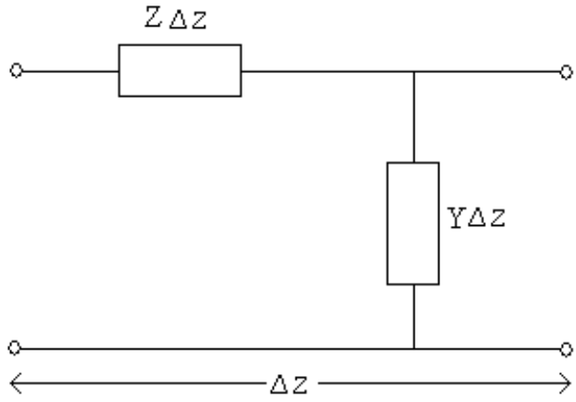

Fig. 1. Transmission line model for an infinitesimal length Δz

For a lossless transmission line the characteristic impedance, Z_0 and the phase constant, β are given by

$$Z_0 = \sqrt{Z/Y} \tag{3}$$

$$j\beta = \sqrt{ZY} \tag{4}$$

Consider now the common transmission line of Fig.2(a), in which the series impedance is an inductance, L Henrys/m and the shunt admittance is a capacitance, C Farads/m .

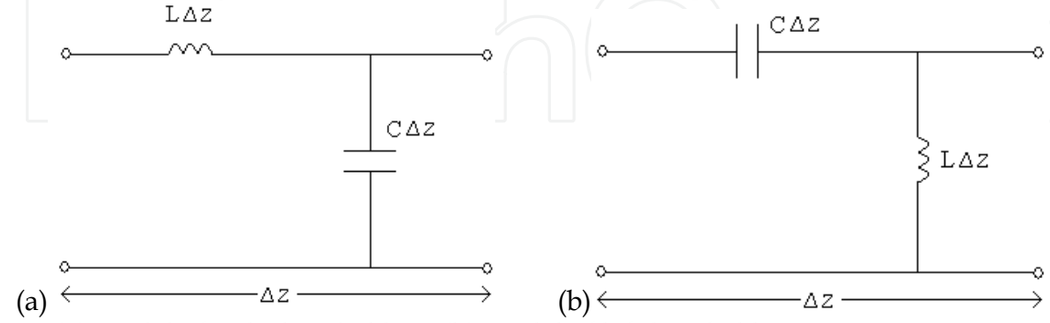

Fig. 2. (a) Model of right-handed line, (b) Model of left-handed line

Noting that $Z = j\omega L$ and $Y = j\omega C$,

$$Z_0 = \sqrt{L/C} \tag{5}$$

$$\beta = \omega\sqrt{LC} \tag{6}$$

The phase velocity is $\omega/\beta = 1/\sqrt{LC}$ and the group velocity is $d\omega/d\beta = 1/\sqrt{LC}$. Both have the same sign and hence are in the same direction. Thus this type of line can represent a right-handed material and is called a right-handed line.

Now consider the transmission line of Fig.2(b), in which the series impedance is a capacitance, C Farads/m and the shunt admittance is an inductance, L Henrys/m . Noting that $Z = 1/j\omega C_\ell$ and $Y = 1/j\omega L_\ell$,

$$Z_0 = \sqrt{L/C} \tag{7}$$

$$\beta = 1/[\omega\sqrt{LC}] \tag{8}$$

The phase velocity is $\omega/\beta = \omega^2\sqrt{LC}$ and the group velocity is $d\omega/d\beta = -\omega^2\sqrt{LC}$.

They are of opposite signs and are therefore in the opposite directions. Hence this type of line can represent a left-handed material and is called a left-handed line.

Two points are to be noted. Firstly, the phase velocity is low at low frequencies when the wave can be regarded as a slow wave. At very high frequencies both phase and group velocities can be arbitrarily large which just indicates that the model cannot be right at high frequencies. The second and most important point for this chapter is that the phase of a right-handed line, proportional to β increases with frequency (in this case linearly). On the other hand, the phase of a left-handed line decreases with frequency (in this case inversely). Although the exact form of variation of β with frequency may not be the same as in the transmission lines considered, the nature of the phase variation is always correct, because $d\omega/d\beta$ is positive for the right-handed line and negative for the left-handed line.

One must now be careful about the word composite in the context of this chapter. For the transmission line, the series impedance may be a series combination of an inductance and capacitance and the shunt admittance can be a parallel combination of an inductance and capacitance. This has the characteristic of a band pass filter. For a certain range of frequencies, the phase has the characteristic of a right-handed line, i.e., it increases with frequency. For another range of frequencies, the phase has the characteristic of a left-handed line, i.e., it decreases with frequency. Such lines showing both types of behaviour have been termed composite-right/left-handed lines (Lai et al, 2004). The composite- right/left-handed line considered in this chapter is a combination of a right-handed line and a left-handed line.

3. Ring Resonators – Single and Dual mode

The microstrip ring resonator was first introduced for measuring dispersion in microstrip lines (Wolff & Knoppik, 1971). However, because of its compact nature, and simplicity of operation, it has been widely used as a resonator in bandpass RF filters. Ring resonators of various shapes – rectangular, square, circular, meander – as well as different types of coupling have been reported. Fig.3 shows a circular microstrip ring resonator.

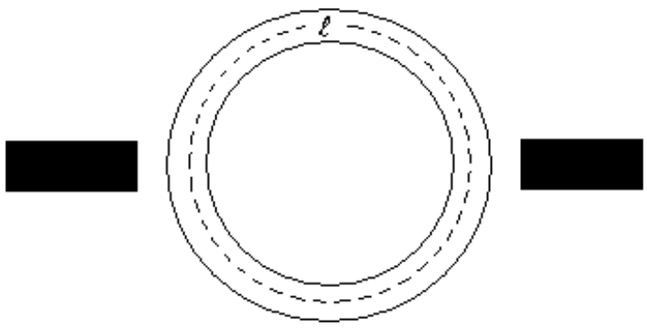

Fig. 3. A single mode microstrip ring resonator with simple microstrip line feeds

The basic principle of operation is that at the resonant frequency, a standing wave exists in the ring. For this to happen, the total phase shift around the ring must be an integer multiple of 2π . If the mean length of the resonator is ℓ , the condition is

$$\beta\ell = 2N\pi \tag{9}$$

where N is an integer and β is the phase constant.

The resonant frequencies are obtained from (9) as

$$f = Nv_p / \ell \tag{10}$$

where, $v_p = 1/\sqrt{LC}$ is the phase velocity of the microstrip line.

For a band pass filter of order n and a symmetric response about the centre frequency, one requires n such resonators each resonant at the centre frequency. The desired frequency response is obtained by the choice of coupling between the resonators. These resonators are called single mode ring resonators, because there is a single resonance at the fundamental frequency. One can on the other hand have two closely spaced resonances near the fundamental. Such ring resonators are called dual mode and were first reported by Wolff (Wolff, 1972). A single dual mode resonator with two close resonant frequencies, f_1 and f_2 is equivalent to two coupled single mode resonators of resonance frequency f_0 and a coupling coefficient

$$k = (f_1 - f_2)/f_0 \tag{11}$$

$$f_0 = \sqrt{f_1 f_2} \tag{12}$$

If one uses dual mode ring resonators, a bandpass filter of order n will require n/2 dual mode resonators as compared to n single mode resonators. This results in a far more compact filter.

A dual mode resonator can be obtained from a single mode resonator design by various ways, such as by having unequal length arms between the feeds, a perturbation in the form

of a notch or patch in one of the arms or by unequal characteristic impedance of the two arms. These are shown in Fig.4.

Fig. 4. Dual mode microstrip line ring resonators: (a) unequal length arms, (b) patch in one arm, (c) notch in one arm, and (d) different characteristic impedances of the arms.

From filter design (Chebyshev, Elliptic etc.) one knows the centre frequency, f_0 as well as the various coupling coefficients. On can then consider replacing a pair of single mode resonator by first calculating f_1 and f_2 using (11) and (12) and the known values of f_0 and the coupling coefficient, k. The mean length of the single mode ring resonator is already known from (10) for the given f_0. Thus one needs to determine the perturbation etc. to obtain the dual mode resonant frequencies f_1 and f_2. Very often the design is obtained by trial and error simulation. However, circuit methods can often provide a good initial design which can then be refined by simulation. Cicuit methods have been extensively discussed by Chang and Hsieh (Chang & Hsieh, 2004).

4. Harmonic Suppression in Bandpass Filters and the Use of Right/Left-handed lines

Unfortunately, many bandpass filters have passbands at the harmonics. This is easy to see in the context of ring resonator filters. Equation (10) shows that the ring resonates at the harmonics. Thus if the coupling between the resonators is constant with frequency, the filter will also have passbands at the harmonics. In practice, the couplings are not constant, but whatever they are, it is expected that the filter will have poor return loss at the harmonics. This is also true of bandpass filters employing dual mode ring resonators. In some applications low attenuation at the harmonics is undesirable.

Several papers report the reduction of harmonic response of ring resonators. One technique (Carroll & Chang, 1994, Karacaoglu et al, 1996, Chang & Hsieh, 2004) is to incorporate a low pass filter in the ring. This filter is built from stepped impedance lines. In Carroll and Chang's resonator, the first harmonic (N=2) was suppressed but with additional loss at the fundamental. In the resonator of Karacaoglu et al, the suppression is 9 dB at the first harmonic and about 6 dB at the second harmonic.

A left-handed line can be incorporated as part of the ring to suppress the first harmonic. As the resonator consists of a right-handed line and a left-handed line, it has been called a composite-right/left-handed line ring resonator (Allen et al, 2006). The principle of operation is completely different from the low pass filter technique and is illustrated in Fig.5.

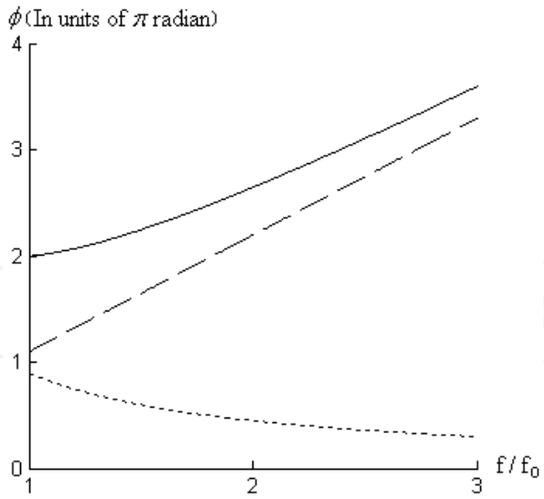

Fig. 5. Phase shifts in the ring resonator. Dashed line: Right-handed line. Dotted line: Left-handed line. Solid line: Total phase shift in the ring

At the resonant frequency, f_0 the phase shift of the right -handed line is φ_R and the phase shift of the left-handed line is φ_L and $\varphi_R + \varphi_L = 2\pi$ as required by ring resonance at the fundamental. According to (6) and (8), the phase shifts vary with frequency as $\frac{f}{f_0}\varphi_R$ for the right-handed line and as $\frac{f_0}{f}\varphi_L$ for the left-handed line. The variation of the phase shifts as well as their sum with the normalized frequency f/f_0 are shown in Fig.5. It is seen that the sum of the phase shifts (solid line) is not 4π at the first harmonic (N=2) as required by ring resonance. This is because the phase of the left-handed line decreases with frequency. Hence the first harmonic is suppressed. However the ring resonance condition can be satisfied at higher frequencies, because the phase shift of the right-handed line increases linearly with frequency while the phase shift of the left-handed line reduces slowly as it is inversely proportional to frequency. However for the suppression of the first harmonic, the precise form of the phase variation of the left-handed line is not important.

5. Implementation of Composite-Right/Left-handed ring resonator

5.1 Left-handed line as an iterative network

Unfortunately, transmission lines with series capacitance are not available. Slow wave structures can be used as left-handed lines only within a range of frequencies. It appears that left-handed metamaterials made with slow wave structures have little to do with filters (Lai et al, 2004). In any case, ring resonators incorporating slow wave structures have not been reported – this may be the subject of future research. Thus a practical way to implement the left-handed line considered here is to use iterative networks made up of lumped series capacitances and lumped shunt inductances. The theory of such networks using the image impedance method is well known (Matthaei et al, 1980). We will consider symmetric

networks for which the two image impedances are equal and are called characteristic impedance. Two types of networks using π and T sections are shown in Fig.6.

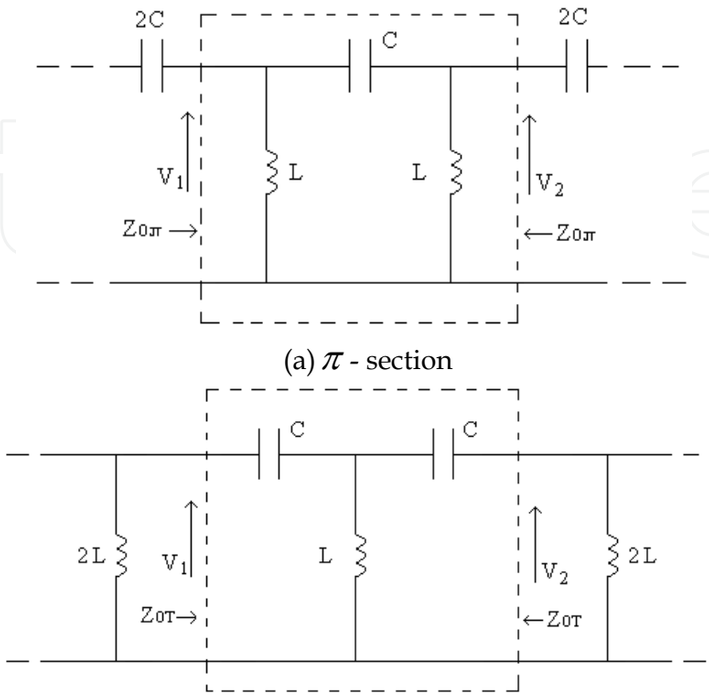

Fig. 6. Left-handed lines represented by iterative networks : (a) π - section, (b) T - section Boxes represent the unit cell of the infinite iterative network

The unit cell (enclosed in the boxes of Fig.6) is a high pass filter. Propagation through a cell is given by

$$V_2 = V_1 \exp(-\Gamma) \tag{13}$$

$$\Gamma = \alpha + j\beta$$

$$\text{and in the passband, } \cos\beta = \left(1 - \omega^2 LC/2\right) \tag{14}$$

For N cells, the phase shift is $N\beta$. The cut-off occurs at $\cos\beta = -1$. The cut-off frequency obtained from (14) is

$$f_c = \frac{1}{\pi\sqrt{LC}} \tag{15}$$

From (14) , it can be shown that

$$\beta = 2\sin^{-1}\frac{f_c}{f} \tag{16}$$

The variation of β against the normalized frequency f/f_c is shown in Fig.7. The phase shift decreases with frequency which is the characteristic of a left-handed line.
The characteristic impedances, $Z_{0\Pi}$ and Z_{0T} are given by

$$Z_{0\Pi} = \sqrt{\frac{L}{C}}\left(1-\frac{f_c^2}{f^2}\right)^{-1/2} \tag{17}$$

$$\text{and } Z_{0T} = \sqrt{\frac{L}{C}}\left(1-\frac{f_c^2}{f^2}\right)^{1/2} \tag{18}$$

The characteristic impedances are imaginary below cut-off and vary widely in the passband.

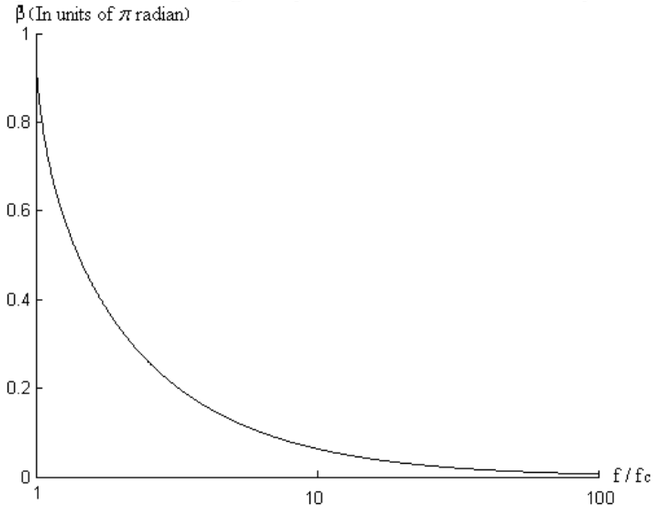

Fig. 7. Variation of the phase, β of a unit cell with frequency

5.2 Incorporating the left-handed line in a ring resonator

The first design is reported by Allen et al (Allen et al, 2006). The schematic diagram of the resonator is shown in Fig.8.

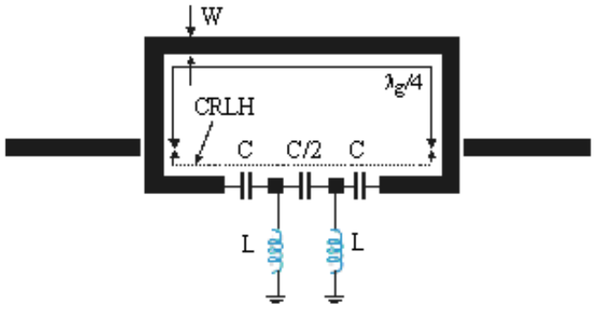

Fig. 8. Ring resonator of Allen et al (From Su & Haldar, 2007, © 2007 IEEE)

The upper part of the resonator is formed by a right-handed (microstrip) line quarter wave long at the centre frequency and of characteristic impedance $50\,\Omega$. For this characteristic

impedance, the width of the microstrip line is W = 1.2 mm for the microstrip substrate of dielectric constant 10.2 and thickness 50 mil. The lower part of the ring is formed by a combination of the microstrip line and the left-handed line. The microstrip line has a total length of 12.3 mm. The left-handed line is formed by two T section unit cells (see Fig.6) with C = 7 pF, L = 8.7 nH. The gap between the input and output lines and the ring resonator is 0.2 mm. The design frequency is 0.88 GHz. The dual mode is said to occur due to the unequal values of the characteristic impedance of the T-section and the 50 Ω characteristic impedance of the microstrip line.

f_c is calculated to be 0.456 GHz. The total phase shift of the lower part of the ring, (the composite-right/left-handed line) is given by

$$\varphi = 2\pi f\sqrt{\varepsilon_{eff}}\,12.3\times10^{-3}\,\ell/c + N\times 2\sin^{-1}(f_c/f) \tag{19}$$

where ε_{eff} is the effective dielectric constant of the microstrip line.

Table 1 shows the phase shift calculated for the upper and lower parts of the resonator and the total phase shift in the ring at the fundamental and harmonics. None of the total phase shifts are integer multiples of 2π. Clearly, (19) can not be employed for resonator design.

Frequency	Phase shift in upper arm (radians)	Phase shift in lower arm eqn. (5) (radians)	Total phase shift around the ring (radians)
f (= 0.88GHz)	0.5π	0.864π	1.364π
2*f*	π	0.675π	1.675π
3*f*	1.5π	0.733π	2.233π

Table 1. Phase shifts along the ring (From Su & Haldar, 2007, © 2007 IEEE)

Fig.9 shows the simulated variation of the magnitude of S_{21} with frequency. There is a peak occuring close to the cut-off frequency.

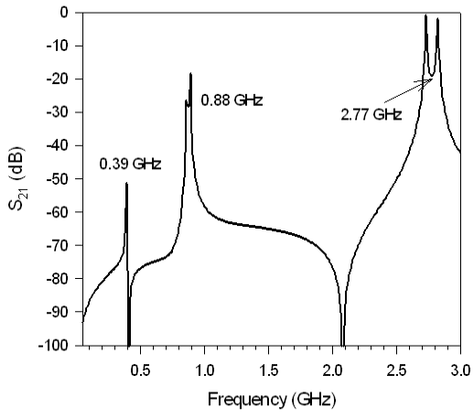

Fig. 9. Variation of the magnitude of S_{21} with frequency for the resonator of Fig.8 (From Su & Haldar, 2007, © 2007 IEEE)

It has been verified by simulation (Su & Haldar, 2007) that an increase in the mismatch of the characteristic impedance of the lines increases the frequency difference of the dual mode and appears to increase the insertion loss between the fundamental and the second harmonic (N=3).

Fig. 10 shows a variation of the resonator. A lower resonant frequency was used to get higher value capacitors to reduce the lower cut-off frequency. The value of the inductor was unchanged. To reduce the number of discrete components, the inductors were replaced by short circuited lines. The length of the line, ℓ is given by

$$\omega_0 L = Z_0 \tan\beta\ell \tag{20}$$

where ω_0 is the resonant frequency, Z_0 and β are the characteristic impedance and propagation constant of the microstrip line implementing the inductor. A large value of Z_0 is preferred to keep the line length short to avoid resonance of the line till about the third harmonic.

Fig.11 shows the simulated variation of the magnitude of S_{21} with frequency. It is interesting to note that harmonics upto the second harmonic (N=3) have been suppressed. The composite ring resonator can suppress several harmonics if the phase shift in the ring at the fundamental is produced mainly by the left-handed line.

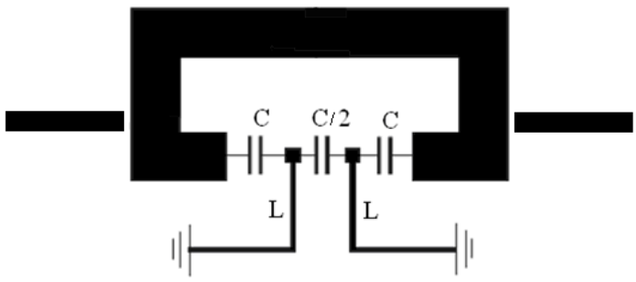

Fig. 10. Redesigned resonator at lower frequency (From Su et al, 2008, © 2008 IEEE)

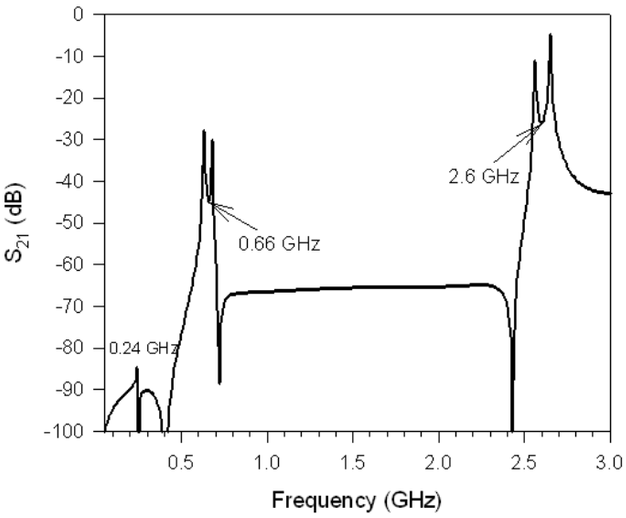

Fig. 11. Variation of the magnitude of S_{21} with frequency for the resonator of Fig.10 (From Su et al, 2008, © 2008 IEEE)

6. Filter design using circuit modelling and simulation of composite-right/left-handed line ring resonators

Table 1 in section 5.2 shows that although the principle of operation is valid, the infinitely extended iterative T- sections theory cannot model the resonator operation well. The size of the resonator limits the number of T and π sections. Many of the reported designs appear to have been carried out by simulation and multi-resonator filters are rarely reported. Circuit models (Chang, 2004) can provide an initial design, which can be refined by simulation.

The authors' intention is to reduce the number of lumped elements. Hence a π -section is used. Fig.12(a) shows the ring resonator with a π -section. The corresponding microstrip version is shown in Fig.12(b). The inductors are implemented with short-circuited transmission lines. Thus the circuit uses only one discrete element.

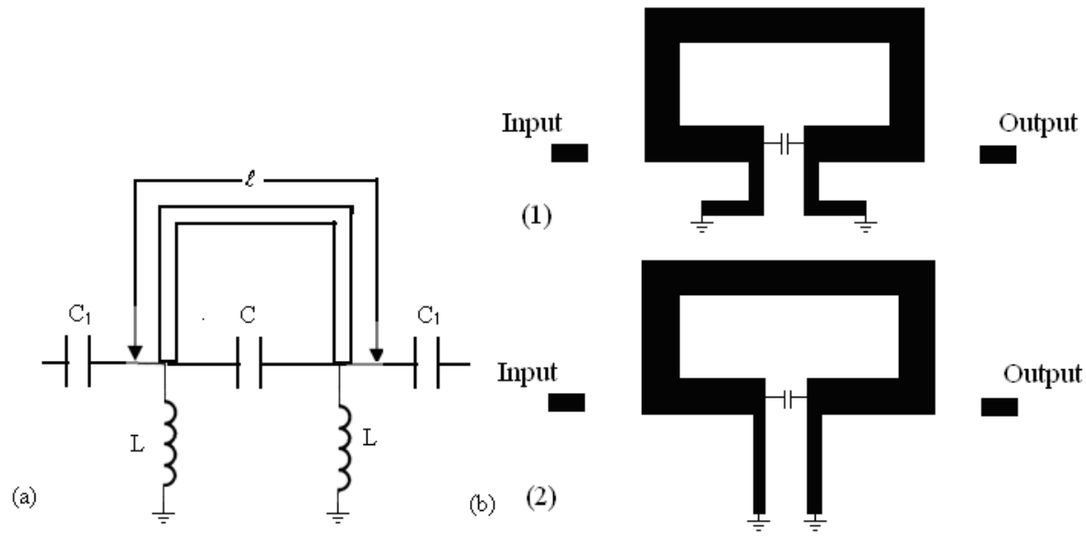

Fig. 12. (a) Circuit model of a ring resonator incorporating a π -section with weak coupling to RF input and output (b) Microstrip layout (From Fong et al, 2009)

Consider the microstrip transmission line of length ℓ, characteristic admittance $Y_{0\ell}$ and propagation constant β, in parallel with the π -section. The Y-parameter of the transmission line considered as a 2-port network is given by

$$Y = \begin{bmatrix} -jY_{0\ell}\cot(\beta\ell) & \dfrac{jY_{0\ell}}{\sin(\beta\ell)} \\ \dfrac{jY_{0\ell}}{\sin(\beta\ell)} & -jY_{0\ell}\cot(\beta\ell) \end{bmatrix} \tag{21}$$

The Y-parameter of the π - section is given by

$$Y = \begin{bmatrix} \frac{1}{j\omega L} + j\omega C & -j\omega C \\ -j\omega C & \frac{1}{j\omega L} + j\omega C \end{bmatrix} \tag{22}$$

For the two networks in parallel, the overall Y-matrix is given by the sum of the Y matrices as follows

$$Y = \begin{bmatrix} -Y_{0\ell}\cot(\beta\ell) + \frac{1}{j\omega L} + j\omega C & \frac{jY_{0\ell}}{\sin(\beta\ell)} - j\omega C \\ \frac{jY_{0\ell}}{\sin(\beta\ell)} - j\omega C & -Y_{0\ell}\cot(\beta\ell)\frac{1}{j\omega L} + j\omega C \end{bmatrix} \tag{23}$$

The resonant frequencies are obtained by setting the determinant of (23) to zero. From the resulting quadratic equation, one can show that the resonant frequencies, ω_1 and ω_2 satisfy the equations

$$\frac{2\omega_1^2 LC - 1}{\omega_1\omega_2 L^2} = Y_{0\ell}^2 \tag{24}$$

$$\frac{1}{\omega_2 L} = Y_{0\ell}\tan(\beta\ell/2) \tag{25}$$

These equations allow one to design dual mode resonators required by a filter design. For example consider the design of a fourth order Chebyshev filter with a centre frequency, f_0 of 0.6 GHz, 10 % fractional bandwidth and a passband ripple of 0.5 dB. This would require four single mode resonators with resonant frequency f_0 with coupling coefficients between resonators 1 and 2 and between 3 and 4, $K_{12} = K_{34} = 0.07$. Resonators 1 and 2 can be replaced by a single dual mode resonator and resonators 3 and 4 can be replaced by an identical dual mode resonator. One now has to design a dual mode resonator with the required coupling coefficient and then couple two such resonators for the required coupling coefficient of $K_{23} = 0.06$. Finally one designs the load and source coupling to get the required external quality factor.

The resonant frequencies of the dual modes are calculated from (11) and (12) using the values of f_0 and K_{12}. Then choosing a standard value of 10 pF for the capacitor, C, the required value of L is calculated from (24) to be 12.9 nH and 4.4 nH. The smaller value is chosen as both lumped inductors and short-circuited transmission lines have higher self-resonant frequencies for lower inductance values. Using (20), this value is implemented by a short-circuited transmission line of characteristic impedance 50 Ω and length 9.8 mm (width is 1.2 mm). The characteristic impedance of the right-handed transmission line is chosen as 28 Ω. RT/Duroid 6010.2 from Rogers Corporation is chosen as the substrate. The width of

the line is calculated to be 3.2 mm. After determining the effective dielectric constant, the length ℓ of the line is then calculated from (24) to be 61.5 mm.

To check the circuit model against simulated results (SONNET, 2008) weak coupling to input and output are used to obtain sharp resonance peaks. For the circuit model of Fig.12(a), this coupling is produced by the small coupling capacitor, C_1 = 0.05 pF. For the microstrip implementations of Fig.12(b) the weak coupling is provided by the gaps. To obtain the response of the circuit, the Y-matrix of the resonator is converted to Z-matrix, added to the Z-matrix of the coupling capacitors and then reconverted to Y-matrix. S_{21} for reference impedance of $50\,\Omega$ ($Y_0 = 1/50\,S$) is calculated from this Y-matrix using

$$S_{21} = \frac{-Y_{21}Y_0}{(Y_{11}+Y_0)(Y_{22}+Y_0)-Y_{12}Y_{21}} \tag{26}$$

Fig.13. compares the variation of the magnitude of S_{21} with frequency for the circuit model and simulations of Fig.12 (b) (1) and (2).

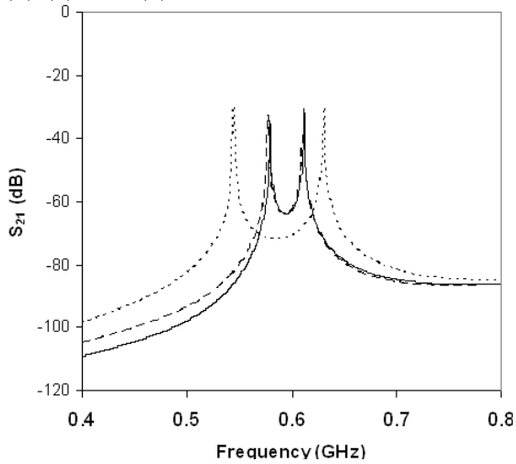

Fig. 13. Comparison of circuit model and simulation. Solid line: circuit model. Dashed line: Fig.12(b)(1). Dotted line: Fig12(b)(2) (From Fong et al, 2009)

Good agreement is obtained between the circuit model and the simulation of Fig.12 (b) (1). The difference with the simulation of Fig.12(b) (2) is ascribed to capacitive coupling between the short circuited lines. To offset this, the inductances of the lines have to be increased by increasing their lengths. Good agreement is obtained when the lengths are increased to 10.8 mm.

For the Chebyshev filter, the required external quality factor, $Q_{ext} = 16.7$. The coupling is obtained by tapping one of short-circuited lines at the source end and at the load end. The resistance in parallel with the inductance is obtained from

$$Q_{ext} = \frac{R}{\omega_0 L} \tag{27}$$

The calculated value of R is 276.3 Ω . An inductor tap transforms the resistance R to 50 Ω load/source impedance. The approximate formula (for high quality factor) is

$$R = 50\left(\frac{L}{L_T}\right)^2 \tag{28}$$

where, L_T is the inductance value at the tap.

The tap position is then given by

$$R = 50\left(\frac{\ell}{\ell_T}\right)^2 \tag{29}$$

where the lengths ℓ and ℓ_T are measured from the short circuit.

Equation (29) is approximate because inductance of a short-circuited line does not vary linearly with length (see equation 20). However, this is adequate because the circuit model establishes an initial design, which is fine tuned by simulation. The gap between two resonators is adjusted to get the filter. Fig. 14 shows a picture of the 4-pole Chebyshev filter. Fig. 15 and 16 show measured and simulated results for the filter.

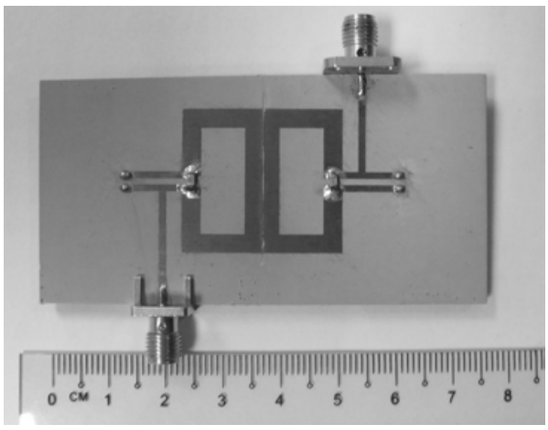

Fig. 14 A picture of the 4-pole Chebyshev filter.

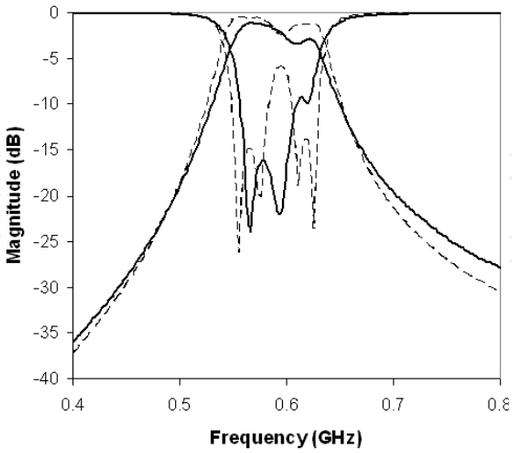

Fig. 15. Variation of magnitudes of S_{21} and S_{11} with frequency. Measured: Solid lines. Simulated (with losses): Dashed lines (From Fong et al, 2009)

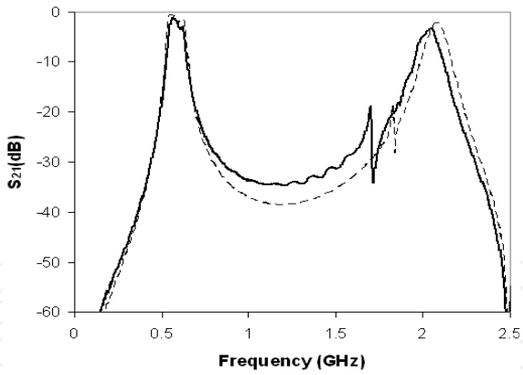

Fig. 16. Wideband frequency response showing harmonic reduction. Measured: Solid line. Simulated: Dashed line (From Fong et al, 2009)

7. Other considerations for composite-right/left-handed line ring resonators

7.1 Practical considerations for lumped capacitors

The reader might have noticed that the centre frequency of the filter designed is quite low. This is a very conservative design to avoid the self resonances of the lumped capacitor. However, it is possible to design for higher frequencies by using the circuit model of the capacitor. Such a circuit model is shown in Fig. 17.

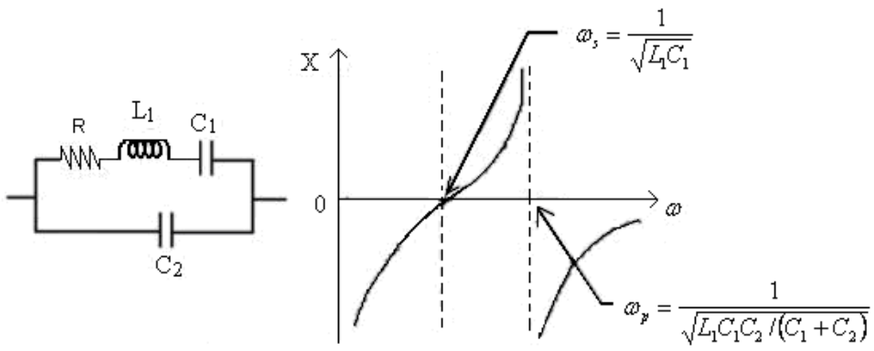

Fig. 17. Capacitor model: (a) Equivalent Circuit (b) Variation of reactance with frequence (ignoring R) showing the series and parallel resonant frequencies. (From Su et al, 2008, © 2008 IEEE)

The model parameters can be obtained by measuring the variation of the S-parameters with frequency and then adjusting the element values of the model to get best agreement with the calculated and measured results. For example, for the 10 pF capacitor considered here, C_1 = 4.22 pF, C_2 = 5.78 pF, R = 0.06 Ω and L_1 = 0.42 nH. The capacitor behaves as a capacitor below the series resonant frequency. So it appears that resonator design using lumped capacitors is limited to frequencies below the series resonant frequency.

Lumped inductors are rarely as good as lumped capacitors both in terms of self resonance and quality factor. Thus when lumped inductors are used, the maximum frequency of

operation may be limited further. Fortunately, they can be replaced by short-circuited transmission lines, but one needs to be careful about the effect resonance of the line on harmonic suppression.

7.2 Tunable composite-right/left-handed line ring resonators

Tunable resonators have been reported by Allen et al (Allen et al, 2007). A typical design is shown in Fig.18. As in their earlier work (Allen et al, 2006), two T sections are used with the two capacitors of each section are replaced by varactor diodes. The dc bias is provided through high characteristic impedance lines with shunt radial stubs.

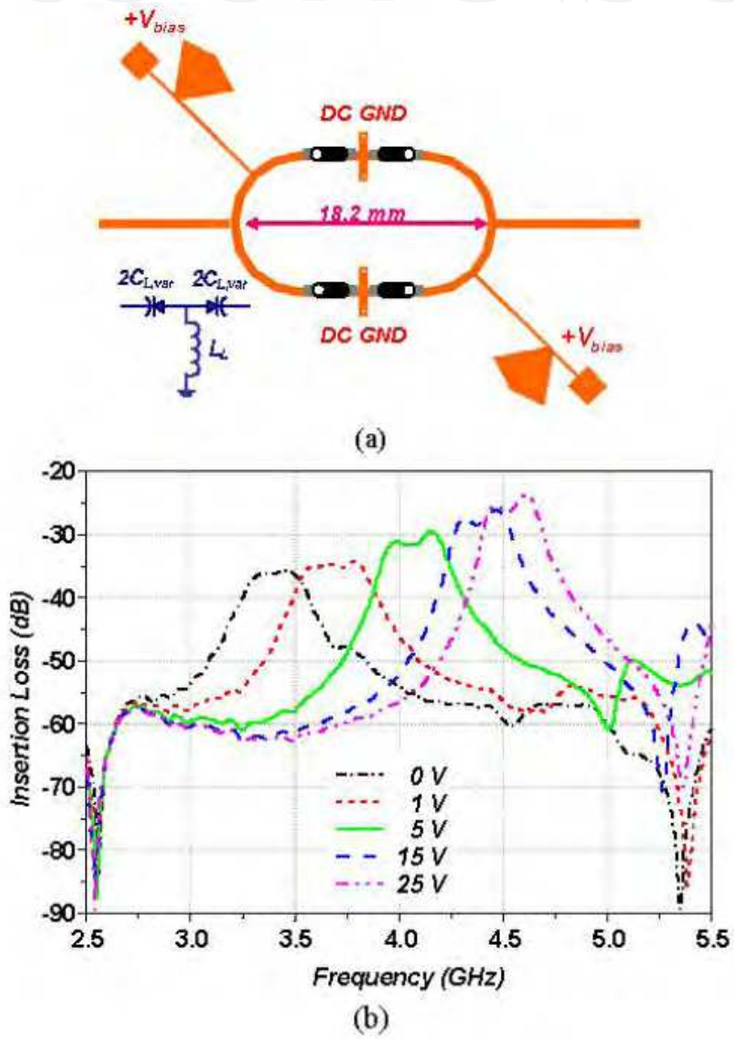

Fig. 18. Tunable resonator (a) Layout (b) Variation of insertion loss with frequency for different bias voltages (From Allen et al, 2007 © 2007 IEEE)

From Fig.18(b), one can see that the centre frequency of the resonator can be shifted by using varactor diodes.

8. Conclusion and future developments

Starting with the explanation of right/left-handed lines, the authors have described recent developments in Dual Mode Microstrip Ring Resonator with Composite-Right/Left-handed Lines. The authors have discussed a circuit technique for the analysis and design. It is shown that a large number of T or π sections may not be needed – the authors describe a resonator with only one π section requiring just one capacitor. However such a section has DC short circuits at both ends of the capacitor. Hence the section is not suitable for designing tunable filters in which dc biased varactor diodes replace capacitors. The design of filters using ring resonators with composite-right/left-handed lines has been explained and demonstrated.

What are the future developments?
Possible developments are as follow:

(1) Can one design compact higher order filters?
(2) Can one use lumped capacitors and inductors near their resonant frequencies to design ring resonators with Composite-Right/Left-handed Lines? It may be possible to use the parallel resonance of a capacitor.
(3) Can one use slow wave structures to replace lumped capacitors for ring resonator with Composite-Right/Left-handed Lines.
(4) Can one design ring resonators with composite-Right/Left-handed Lines using coplanar transmission lines?

9. References

Allen, C.A.; Leong, K.M.K.H. & Itoh, T. (2006). Dual-mode composite-right/left-handed transmission line ring resonator. *Electronics Letters,* 42, 2, (2006) pp. 96-97, ISSN: 0013-5194.

Allen, C.A.; Leong, K.M.K.H. & Itoh, T. (2007). Fixed frequency and tunable metamaterial based ring resonators with narrowly spaced resonances , *Microwave Symposium Digest, IEEE MTT-S International*, pp. 1623-1626, ISBN:1-4244-0688-9, Honolulu, USA, June, 2007.

Beck, A.H.W (1958). *Space Charge Waves,* Pergamon Press, New York

Carroll, J.M. & Chang K. (1994) Microstrip mode suppression ring resonator. *Electronics Letters,* 30, 22, (1994) pp.1861-1862, ISSN: 0013-5194

Chang, K. & Hsieh, L.H. (2004). *Microwave Ring Circuits and Related Structures,* John Wiley & Sons. Inc, ISBN: 978-0-471-44474-9, New York

Fong, K.K. ; Su, H.T. & Haldar, M.K. (2009). Circuit modelling for the design of composite-right/left-handed ring resonator, Submitted to *2009 Asia Pacific Microwave Conference*, Singapore, December, 2009.

Karacaoglu, U.; Sanchez-Hernandes, D. ; Robertson, I.D. & Guglielmi, M. (1996). Harmonic suppression in microstrip dual-mode ring-resonator bandpass filters, *Microwave Symposium Digest, IEEE MTT-S International*, pp. 1635-1638, ISBN:0-7803-3246-6, conference location, June, 1996.

Lai, A.; Itoh, T. & Caloz, C. (2004). Composite Right/Left-Handed Transmission Line Metamaterials. *IEEE Microwave Magazine,* Vol., No., (2004) pp.34-50), ISSN:1527-3342.

Matthaei, G.; Young, L. & Jones, E.M.T. (1980). *Microwave Filters, Impedance-Matching Networks and Coupling Structures,* Artech House, ISBN: 0-89006-099-1, Norwood, MA (USA).

Shelby, R.A.; Smith, D.R. & Schultz, S. (2001). Experimental verification of negative index of refraction. *Science,* Vol.292, No.5514, (2001) pp.77-79, ISSN 0036-8075 (print), 1095-9203 (online).

SONNET 11.52 Sonnet Software Inc., Pittsburgh, PA, 2008.

Su, H.T. & Haldar, M.K. (2007). Redesign of a dual-mode ring resonator using composite-right/left-handed line, *2007 Asia Pacific Microwave Conference*, pp. 2269-2272, ISBN: 978-1-4244-0748-4, Bangkok, December, 2007.

Su, H.T. ; Fong, K.K. ; Haldar, M.K. & Wong, M.L.D. (2008). New 4-pole dual-mode resonator using composite-right/left-handed line, *2008 Asia Pacific Microwave Conference*, pp. 1-4, ISBN: 978-1-4244-2641-6, Hong Kong, China, December, 2008.

Vaselago, V.G. (1968). The electrodynamics of substances with simultaneously negative values of ε and μ . *Soviet Physics Uspekhi,* 10, 4, (1968) ppp.509-514, ISSN: 0038-5670

Wolff, I. & Knoppik, N (1971). Microstrip bandpass filter using degenerate modes of a microstrip ring resonator. *Electronics Letters,* 7, 26, (1971) pp. 779-781, ISSN: 0013-5194.

Wolff, I. (1972). Microstrip ring resonator and dispersion measurements on microstrip lines. *Electronics Letters,* 8, 12, (1972) pp.302-303, ISSN: 0013-5194.

IntechOpen

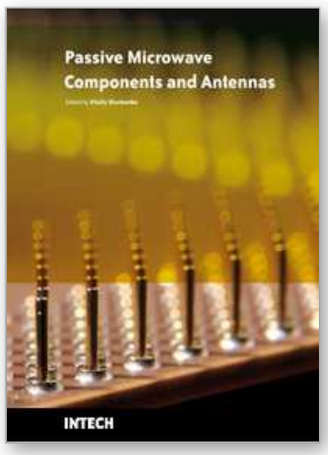

Passive Microwave Components and Antennas

Edited by Vitaliy Zhurbenko

ISBN 978-953-307-083-4
Hard cover, 556 pages
Publisher InTech
Published online 01, April, 2010
Published in print edition April, 2010

Modelling and computations in electromagnetics is a quite fast-growing research area. The recent interest in this field is caused by the increased demand for designing complex microwave components, modeling electromagnetic materials, and rapid increase in computational power for calculation of complex electromagnetic problems. The first part of this book is devoted to the advances in the analysis techniques such as method of moments, finite-difference time- domain method, boundary perturbation theory, Fourier analysis, mode-matching method, and analysis based on circuit theory. These techniques are considered with regard to several challenging technological applications such as those related to electrically large devices, scattering in layered structures, photonic crystals, and artificial materials. The second part of the book deals with waveguides, transmission lines and transitions. This includes microstrip lines (MSL), slot waveguides, substrate integrated waveguides (SIW), vertical transmission lines in multilayer media as well as MSL to SIW and MSL to slot line transitions.

InTech Europe
University Campus STeP Ri
Slavka Krautzeka 83/A
51000 Rijeka, Croatia
Phone: +385 (51) 770 447
Fax: +385 (51) 686 166
www.intechopen.com

InTech China
Unit 405, Office Block, Hotel Equatorial Shanghai
No.65, Yan An Road (West), Shanghai, 200040, China
中国上海市延安西路65号上海国际贵都大饭店办公楼405单元
Phone: +86-21-62489820
Fax: +86-21-62489821

IntechOpen